Pth1/Vam3p Is the Syntaxin Homolog at the Vacuolar Membrane of *Saccharomyces cerevisae* Required for the Delivery of Vacuolar Hydrolases

Amit Srivastava and Elizabeth W. Jones

Department of Biological Sciences, Carnegie Mellon University, Pittsburgh, Pennsylvania 15213

Manuscript received August 18, 1997
Accepted for publication September 29, 1997

ABSTRACT

The *PEP12* homolog Pth1p (Pep twelve homolog 1) is predicted to be similar in size to Pep12p, the endosomal syntaxin homolog that mediates docking of Golgi-derived transport vesicles and, like other members of the syntaxin family, is predicted to be a cytoplasmically oriented, integral membrane protein with a C-terminal transmembrane domain. Kinetic analyses indicate that Δ*pth1*/*vam3* mutants fail to process the soluble vacuolar hydrolase precursors and that PrA, PrB and most of CpY accumulate within the cell in their Golgi-modified P2 precursor forms. This is in contrast to a *pep12* mutant in which P2CpY is secreted from the cell. Furthermore, *pep12* is epistatic to *pth1*/*vam3* with respect to the CpY secretion phenotype. Alkaline phosphatase, a vacuolar membrane hydrolase, accumulates in its precursor form in the Δ*pth1*/*vam3* mutant. Maturation of pro-aminopeptidase I, a hydrolase precursor delivered directly to the vacuole from the cytoplasm, is also blocked in the Δ*pth1*/*vam3* mutant. Subcellular fractionation localizes Pth1/Vam3p to vacuolar membranes. Based on these data, we propose that Pth1/Vam3p is the vacuolar syntaxin/t-SNARE homolog that participates in docking of transport vesicles at the vacuolar membrane and that the function of Pth1/Vam3p impinges on at least three routes of protein delivery to the yeast vacuole.

THE lysosome-like vacuole of *Saccharomyces cerevisae* is an acidic organelle containing an ensemble of cellular hydrolases, including the major proteases carboxypeptidase Y (CpY), proteinase A (PrA), proteinase B (PrB) and the repressible integral membrane alkaline phosphatase (ALP) (Jones and Murdock 1994; Jones *et al.* 1997; Van den Hazel *et al.* 1996). The vacuolar hydrolases are known to catalyze specific limited cleavages necessary for protein maturation; they are also known to be active on a global scale mediating protein turnover in response to the cellular environment (Jones 1991; Jones and Murdock 1994; Jones *et al.* 1989; Jones *et al.* 1997; Van den Hazel *et al.* 1996). The vacuole plays an important role in ion homeostasis and also acts as a repository for polyphosphate, amino acids and other small molecules (Wiemken and Durr 1974; Wiemken *et al.* 1979; Urech *et al.* 1978; Cooper 1982; Ohsumi and Anraku 1983; Serrano 1991; Dunn *et al.* 1994).

The vacuole receives proteinaceous cargo in a variety of ways. Soluble hydrolases like PrA, PrB and CpY, travel through the early stages of the secretory pathway—from the endoplasmic reticulum (ER) to the Golgi; they are actively sorted away from the secretory bulk flow in a late-Golgi compartment and then reach the vacuole via the prevacuolar endosome-like compartment (Stevens *et al.* 1982; Jones *et al.* 1997). In a Δ*vps1* mutant, in which the vacuolar branch of the secretory pathway is blocked, the precursor of vacuolar membrane hydrolase ALP travels to the vacuole via the plasma membrane and the endocytic pathway (Nothwehr *et al.* 1995). However, the evidence indicates that ALP normally travels to the vacuole via a pathway that does not involve either the plasma membrane or the prevacuole/endosome; direct delivery from the Golgi to the vacuole has even been suggested (Cowles *et al.* 1997; Webb *et al.* 1997). The vacuolar hydrolases α-mannosidase (Yoshihisa and Anraku 1990) and aminopeptidase I (ApI) (Klionsky *et al.* 1992) reach the vacuole directly from the cytoplasm independent of the secretory pathway.

Mutants defective in vacuolar biogenesis and/or function have been recovered in several screens and selections: *pep*, defective in vacuolar peptidase activity (Jones 1977); *vps*, defective in protein sorting to the vacuole (Bankaitis *et al.* 1986; Robinson *et al.* 1988; Rothman and Stevens 1986; Rothman *et al.* 1989); or *vam*, abnormal vacuolar morphology (Wada *et al.* 1992). Along with a few other mutants, these mutants define over 40 complementation groups, with extensive genetic overlap among mutant collections. These complementation groups identify molecular components that are involved in trafficking between the Golgi and the vacuole and/or in maintaining integrity of the vacuolar compartment.

Intracellular protein translocation between membrane-bound organelles has been shown to occur using transport vesicles that employ a set of proteins designated as the "SNARE complex" to ensure docking fol-

Corresponding author: Amit Srivastava, Department of Biological Sciences, Carnegie Mellon University, Mellon Institute, 4400 Fifth Avenue, Pittsburgh, PA 15213. E-mail: amits@cmu.edu

lowed by fusion at the appropriate target organelle (Rothman 1994). The specificity of docking is believed to be achieved by interaction between the specific v-SNAREs/synaptobrevins and t-SNAREs/syntaxins on the vesicle and target membranes, respectively. Ancillary factors such as NSF, SNAP, Sec1p and SNAP-25 homologs assemble around the two SNAREs to accomplish fusion in an ATP-dependent manner. Members of the Rab family of small GTP-binding proteins are believed to participate in regulation of the docking and fusion reaction (Pryer *et al.* 1992; Rothman 1994; Sudhof 1995). Functional homologs of the SNARE complex proteins have been found at almost every stage of the secretory pathway and its vacuolar branch, testifying to the notion that trafficking between the Golgi and the vacuole makes use of transport vesicles (Bennet and Scheller 1993; Ferro-Novick and Jahn 1994; Jones *et al.* 1997).

Our laboratory has previously reported the identification and characterization of a syntaxin homolog, Pep12p, that functions at the first step of the vacuolar branch of the secretory pathway mediating docking and/or fusion of Golgi-derived transport vesicles at the prevacuolar endosome-like compartment (Becherer *et al.* 1996). In this article we report the identification and characterization of a member of the syntaxin family that functions at the second and final step of the vacuolar protein targeting pathway. Pth1p (Pep twelve homolog 1) was identified in a genome database search for new members of the yeast syntaxin family using the heptad repeat region of Pep12p, which is the most highly conserved region among the syntaxins. In the absence of Pth1p, delivery of hydrolases to the vacuole is impaired, implicating it in the vacuolar protein targeting pathway.

MATERIALS AND METHODS

Materials: Restriction enzymes and T4 DNA ligase were purchased from Boehringer Mannheim Biochemicals (Indianapolis, IN) and were used according to manufacturer's instructions. Taq DNA polymerase was purchased from Fisher Scientific (Pittsburgh, PA). Lyticase L-8012, β-glucuronidase G-7770 and Ponceau S were obtained from Sigma Chemical Co. (St. Louis, MO). Protein A–Sepharose CL4B was purchased from Pharmacia (Piscataway, NJ). Trans^{35}S was purchased from ICN Biochemicals (Costa Mesa, CA). Goat anti-rabbit IgG-HRPO conjugate was purchased from Bio-Rad (Hercules, CA). Nitrocellulose membrane "Optitran" type HA85 was obtained from Schleicher & Schuell (Keene, NH). Other chemicals were from Sigma Chemical Company, standard sources, or as indicated. Oligonucleotide primers were obtained from Ransom Hill Bioscience (Ramona, CA). Anti-HA 12CA5 monoclonal antibodies were purchased from Boehringer Mannheim Biochemicals. Antibodies to glucose-6-phosphate dehydrogenase (G6PDH) were purchased from Sigma Chemical Company. We are thankful for the kind gifts of antibodies to the following proteins: Pep12p and ALP for immunoprecipitation from S. Emr; ALP for immunoblot from G. Payne; Kex2p from R. Fuller and ApI from D. Klionsky.

Media and strains: YPD and synthetic yeast media (Jones *et al.* 1982) and LB medium (Sambrook *et al.* 1989) were prepared as described previously. Ampicillin (Sigma) was used at 100 μg/ml. YPD, 0.5 m K_2HPO_4 pH 7 medium was prepared as follows: YP (yeast extract and peptone) solution, dextrose solution and the buffer were autoclaved in separate flasks; the three solutions were mixed aseptically just before pouring plates (Preston *et al.* 1989). Media containing various concentrations of divalent cations ($ZnCl_2$, $CaCl_2$, $SrCl_2$, $MnCl_2$, LiCl, NaCl) were prepared by autoclaving YPD medium and the stock salt solutions separately; after cooling to 55°, the appropriate amount of salt solution was added to achieve the desired concentration (Webb *et al.* 1997). Standard genetic methods were used (Hawthorne and Mortimer 1960). The Δ*pth1*-associated CpY deficiency was scored by the *N*-acetyl-dl-phenylalanine-β-napthyl ester (APE) overlay plate assay (Jones 1977).

All yeast strains were derived in our laboratory from strain X2180-1B (*MAT*α *gal2 SUC2*) or from crosses between strains in our isogenic series and strains congenic to strain X1280-1B that we obtained from D. Botstein or P. Hieter. The strains and their genotypes are given in Table 1. All plasmids were propagated in the strain LM1035 (Cepko *et al.* 1984).

Nucleic acid preparation and manipulation: Bacterial plasmid DNA was extracted by the alkaline lysis method of Birnboim and Doly (1979) and used directly. The $CaCl_2$ method was used for bacterial transformation (Sambrook *et al.* 1989). The lithium acetate/dimethyl sulfoxide method was used for yeast transformation (Hill *et al.* 1991). Yeast genomic DNA was prepared by the method of Hoffman and Winston (1987), as was the plasmid DNA that was isolated from yeast to be shuttled into *Escherichia coli*. Polymerase chain reaction (PCR) was carried out by standard methods in a Perkin-Elmer Cetus thermal cycler. The techniques for preparation and analysis of DNA fragments have been described previously (Sambrook *et al.* 1989). After electrophoresis in 1% agarose gels run in TBE buffer, staining in ethidium bromide and visualization by the use of long-wave UV light, gel slices containing DNA fragments were excised from agarose gels and DNA was extracted using a QIAGEN gel extraction kit (Santa Clarita, CA) following the manufacturer's instructions.

Plasmid constructions: A null allele of *PTH1* was constructed by replacing the entire open reading frame (ORF) with the *HIS3* gene using the PCR deletion technique (Baudin *et al.* 1993). pBJ8793 carrying a 2.4-kb *Eco*RI–*Bam*HI genomic DNA fragment bearing *PTH1* was constructed as follows: using the sequence from the Saccharomyces Genome Database (SGD), primers against regions approximately 540 nt upstream and 1050 nt downstream of YOR106w were synthesized. PCR on genomic DNA yielded a 2.4-kb amplification product with restriction sites at each end introduced by the primers. The amplification product was digested with *Eco*RI and *Bam*HI; the restriction fragment was gel purified and then cloned into the corresponding sites of single and high copy plasmids of the pRS series (Sikorski and Hieter 1989).

Epitope tagging of Pth1p: Construction of a HA-tagged version of *PTH1* was carried out as follows: an *Eco*RI site was introduced by PCR immediately before the first ATG codon of the *PTH1* ORF. A *Xho*I site was introduced by PCR approximately 830 bp downstream of the stop codon. The PCR amplification product obtained by using the *Eco*RI and *Xho*I primers was digested using the same enzymes and the restriction fragment was ligated into the *Eco*RI and *Xho*I sites in the HA-tagging vector pRD54 GAL1::HA in pRS316 (constructed by R. Deshaies) yielding the plasmid pBJ9068 with a single copy of the HA epitope fused in frame at the 5′ end of the *PTH1* ORF; the ATG for the fusion is provided by the HA epitope. The 670 bp *GAL1* promoter in pBJ9068 was completely re-

TABLE 1

Yeast strains

Strain	Genotype	Source
BJ5414	*MAT***a** *his3Δ200 ura3-52 lys2-801 trp1Δ101*	Laboratory strain
BJ6252	*MATα his3Δ200 ura3-52 leu2Δ1*	Laboratory strain
BJ8765	*MAT***a**/*MATα Δpth1::HIS3*/+ *his3Δ200*/+ *ura3-52*/*ura3-52 leu2Δ1*/+ *lys2-801*/+ *trp1Δ101*/+	This study
BJ8771	*MATα Δpth1::HIS3 his3Δ200 ura3-52 leu2Δ1 lys2-801*	This study
BJ8776	*MATα Δpth1::HIS3 his3Δ200 ura3-52 leu2Δ1 lys2-801 trp1Δ101*	This study
BJ8917	*MATα pep4-3 his3Δ200*	Laboratory strain
BJ8922	*MAT***a** *pep12::LEU2 his3Δ200 ura3-52 leu2Δ1 trp1Δ101*	This study
BJ8926	*MATα his3-Δ200 ura3-52 leu2Δ1*	This study
BJ8927	*MATα Δpth1::HIS3 his3-Δ200 ura3-53 leu2Δ1*	This study
BJ8928	*MAT***a** *pep12::LEU2 his3-Δ200 ura3-52 leu2Δ1 lys2-801 trp1Δ101*	This study
BJ8929	*MAT***a** *Δpth1::HIS3 pep12::LEU2 his3-Δ200 ura3-52 leu2Δ1 lys2-801 trp1Δ101*	This study

placed with the native upstream region of *PTH1* (without adding any extraneous sequence) as follows: the 540 bp region upstream of the *PTH1* ORF was amplified flanked by the restriction sites, *Xba*I and *Bam*HI, introduced by PCR; the fragment was cloned into the corresponding sites of pBJ9068, resulting in the plasmid pBJ9070. For introduction of the triple HA tag, *Eco*RI sites were engineered by PCR on both ends of a 121 bp DNA fragment encoding the triple HA epitope (kind gift from B. Futcher, Cold Spring Harbor Laboratory, Cold Spring Harbor, NY, and S. Michaelis, Johns Hopkins University, Baltimore, MD). The amplification product was digested with *Eco*RI and then ligated into the *Eco*RI site between the resident single HA tag and the first ATG of the *PTH1* ORF in pBJ9070. Orientation of the triple tag was checked by PCR followed by testing the ability to complement the Δ*pth1* mutation. The plasmid pBJ9100 satisfied both criteria. This HA-tagged version of *PTH1* could be detected in immunoblots and also by immunoprecipitation from radiolabeled whole-cell protein extracts; no corresponding protein band was observed in strains carrying the vector alone.

Spheroplast labeling and immunoprecipitation: Radiolabeling of spheroplasts was carried out as described in Webb *et al.* (1997). In brief, cells were grown to early log phase in Wickerham's minimal (WM) medium, 4–6 OD_{600} units of cells/sample were collected and spheroplasts prepared. Spheroplasts were resuspended in labeling medium (WM plus 0.7 m sorbitol plus 1 mg/ml bovine serum albumin), preincubated for 5 min at 30°, pulse labeled at 30° with Trans^{35}S (50 μCi/OD_{600}) for 20 min and chased for 30 min by adding unlabeled methionine, cysteine and yeast extract to final concentrations of 5 mm, 1 mm and 0.2%, respectively. The cultures were then spun for 1 min at 13,000 × *g* to generate intracellular spheroplast and extracellular medium fractions. TCA was added to a final concentration of 8%. The TCA-precipitated protein was pelleted, washed twice with chilled acetone and resuspended in suspension buffer (50 mm, TRIS pH 7.5, 1 mm EDTA, 1% SDS). Proteins were resolubilized by disrupting the pellet by vortexing in the presence of glass beads. Vacuolar hydrolases PrA, PrB, CpY and ALP were immunoprecipitated and then analyzed by SDS-PAGE and autoradiography.

Immunoblots: Yeast protein extracts were subjected to SDS-PAGE. CpY, PrA, ALP and ApI were separated on 10% and PrB on 12% acrylamide gels. Immunoblotting was carried out as described elsewhere (Woolford *et al.* 1990). Immune complexes were detected using goat anti-rabbit IgG-HRPO-conjugated antibodies (Bio-Rad). 4-Chloro-1-naphthol was used as chromogenic substrate.

Subcellular fractionation: Subcellular fractionation by differential centrifugation was carried out as described in Becherer *et al.* (1996).

Electron microscopy: Cells subjected to electron microscopy were processed as described in Webb *et al.* (1997). In brief, cells were grown in YPD to an OD of approximately 0.5 A_{600}. Cells were fixed for 2 hr, washed and then resuspended in the presence of β-glucuronidase and lyticase for 2 hr to allow cell wall removal. After washing, cells were embedded, stained and viewed as previously described (Webb *et al.* 1997).

6-CFDA staining: Cells were labeled with the vital vacuolar stain 6-carboxyfluorescein diacetate (6-CFDA), as described elsewhere (Preston *et al.* 1989).

RESULTS

Identification of a Pep12p homolog: We have previously reported the identification and characterization of Pep12p, a syntaxin or t-SNARE resident in the endosomal membrane that mediates docking and/or fusion of Golgi-derived transport vesicles along the vacuolar protein targeting pathway (Becherer *et al.* 1996). The heptad repeat sequence from Pep12p was used to search the SGD for homologous sequences that might encode syntaxin or t-SNARE proteins involved in similar docking and fusion processes along intracellular protein translocation pathways. An ORF—YOR3220w (old ORF name, current designation: YOR106w) on chromosome *XV* was identified that exhibited 34% identity and 57% similarity with Pep12p. YOR106w is 283 amino acids long with a predicted molecular mass of 32,495 Daltons. The amino acid sequence contains two potential N-linked glycosylation sites. Hydropathy analysis by the method of Kyte and Doolittle (1982) revealed a 20 amino acid long C-terminal hydrophobic region flanked by positively charged residues. YOR106w was thus predicted to be a cytoplasmically oriented integral membrane protein (Figure 1, A and B).

The region between amino acids 226 and 258 of YOR106w (just upstream of the transmembrane domain) contains a heptad repeat that is predicted to

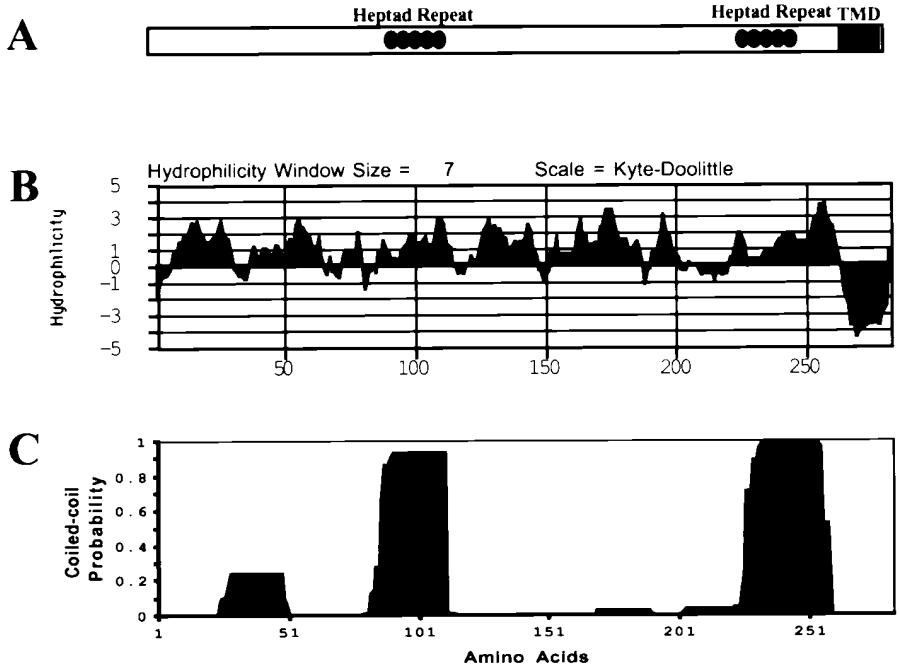

Figure 1.—Features of Pth1p. (A) Like other members of the syntaxin protein family, Pth1p (YOR106w) is predicted to be a 283 amino acid polypeptide with a C-terminal transmembrane domain (TMD) and a heptad repeat just upstream of the TMD (with an additional, more N-terminal heptad repeat region). (B) Hydropathy plot of the predicted Pth1p polypeptide (Kyte and Doolittle 1982). (C) Coiled-coil formation probability generated using the COILS-2.1 program (MTIK matrix, **a** and **d** positions weighted, 21 residue window).

adopt an α-helical coiled-coil conformation. The probability that regions within the amino acid sequence would form coiled coils was calculated using the COILS 2.1 program (McLachlan and Stewart 1975; McLachlan and Karn 1982; Parry 1982; Cohen and Parry 1986; Lupas *et al.* 1991). This putative coiled-coil domain in YOR106w was found in the region most conserved in the syntaxins. The residues at positions **a** and **d** of the heptad repeat are especially conserved within the family and these residues (except two) are identical between Pep12p and YOR106w (Figure 2). An additional heptad repeat exists further upstream of the transmembrane domain between amino acids 86 and 111 and is also strongly predicted to form an α-helical coiled coil by the COILS program (Figure 1, A and C).

In view of the several similarities between Pep12p and YOR106w at the sequence level and also the fact that YOR106w was identified using the heptad repeat region of Pep12p, we decided to name the ORF, Pep twelve homolog 1 or PTH1. [During the course of this work, a GenBank submission identified YOR106w as *VAM3* (Wada *et al.* 1992; Wada *et al.* 1997)].

Deletion of the *PTH1* gene: A null allele of *PTH1* was constructed by replacing the entire ORF with the *HIS3* gene using the PCR deletion technique (Baudin *et al.* 1993) (Figure 3B). Two primers each 60 bases long were synthesized; 41 nt of each primer corresponded to the sequence immediately upstream or downstream of the ORF, followed by a stretch of 19 nt homologous to the *HIS3* selectable marker. Using the primers, along with the cloning vector pRS303 (*HIS3*) (Sikorski and Hieter 1989) as template, PCR amplification was carried out, generating a 1.2 kb amplification product. The amplified DNA molecule contained the entire *HIS3* gene flanked by 40 nt of sequences homologous to the region flanking the *PTH1* ORF. The PCR mixture was used to transform a His^- diploid recipient strain to His^+. This recipient strain (BJ5414/BJ6252) carried the *his3-Δ200* deletion that removes all sequences homologous to the *HIS3* gene used for the

```
        140                       160                       180                       200
Pep12p VNERAKESLEASEMANDAAL LDEEQRQNSSKSTRIPGSQI VIERDPINNEEFAYQQNLIE QRDQE 204
Pth1p  AVRQDPESSYISIKVNEQSP LLHNEGQ---HQLQLQEEQE QQQQ-GLSQEELDFQTIIHQ ERSQQ 199

        205                       225                       245                       264
Pep12p ISNIERGITELNEVFKDLGS VVQQQGVLVDNIEANIYTTS DNTQLASDELRKAMRYQK-R TSRWR 268
Pth1p  IGRIHTAVQEVNAIFHQLGS LVKEQGEQVTTIDENISHLH DNMQNANKQLTRADQHQRDR NKCGK 264
       |  |  |  |  |  |     |  |  |  |  |
       a  d  a  d  a  d     a  d  a  d  a
```

Figure 2.—Sequence alignment of Pep12p and Pth1p (YOR106w) in the heptad repeat region, upstream of the C-terminal transmembrane domain. Identical amino acid residues are in boldface. Overall the two proteins are 34% identical and 57% similar. Pep12p has a heptad repeat region—amino acids 205–245—and the amino acid residues at positions **a** and **d** within this repeat are especially conserved among members of the syntaxin family of proteins. These residues are also conserved in Pth1p, and all but two amino acids are identical between Pep12p and Pth1p.

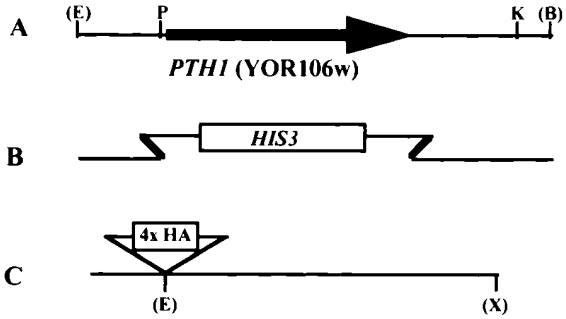

Figure 3.—Characterization, disruption and epitope tagging of the *PTH1* locus. (A) Restriction map of the cloned genomic region of *PTH1* (2.4-kb *Eco*RI/*Bam*HI fragment, pBJ8793) is shown with the 0.849-kb *PTH1* ORF indicated with the solid arrow. E, *Eco*RI; B, *Bam*HI; P, *Pst*I; K, *Kpn*I; X, *Xba*I; parentheses indicate restriction enzyme sites engineered by PCR. The plasmid carrying this insert—pBJ8973 (see Table 2) was able to complement the CpY deficiency of the Δ*pth1::HIS3* mutant (BJ8776, see Table 1). (B) The entire *PTH1* ORF (YOR106w) was replaced with a fragment bearing the *HIS3* gene by PCR deletion (Baudin *et al.* 1993). A strain in which this disruption construct had been integrated into the genome displayed a deficiency in CpY activity. (C) The quadruple HA epitope tag was inserted immediately before the first ATG of the *PTH1* ORF (pBJ9100, see materials and methods; Table 2). This *PTH1::HA* fusion was able to complement the CpY deficiency of the *Δpth1::HIS3* mutant (BJ8776, see Table 1).

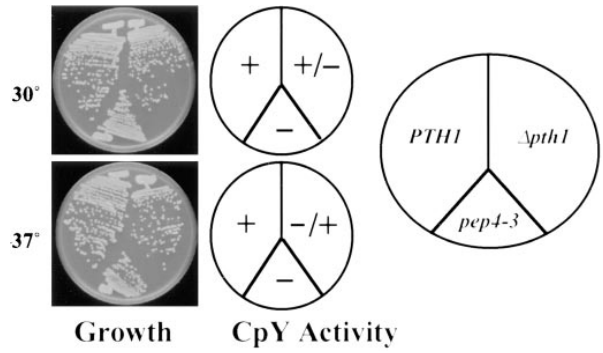

Figure 4.—Effects of deleting *PTH1* on viability and CpY activity at both 30° and 37° were examined. CpY activity of Δ*pth1::HIS3* mutant was assessed by CpY (APE overlay) plate assay (Jones 1977). *PTH1* (BJ6252), *Δpth1::HIS3* (BJ8776), *pep4-3* (BJ8917).

disruption. The solitary His^+ transformant obtained (BJ8765) was sporulated and tetrads were dissected. All four spores of each tetrad grew equally well (at both 30° or 37°), indicating that *PTH1* is not essential for growth and that loss of Pth1p does not cause a growth defect (Figure 4). The spores were tested for CpY activity by means of the APE overlay plate assay (Jones 1977). In 24 tetrads CpY deficiency and His protrophy segregated 2:2, and all His^+ spores were CpY deficient. This was a strong indication that Pth1p function impinged on the vacuolar protein targeting pathway. Closer examination of the CpY deficiency indicated that the Δ*pth1::HIS3* mutant displayed a level of CpY activity intermediate between the positive (*WT*) and negative (*pep4-3*) controls. The CpY deficiency phenotype was more pronounced at 37° (Figure 4).

Cloning of the *PTH1* gene: Using the sequence obtained from the *S. cerevisiae* genome sequencing project, the *PTH1* gene was cloned by genomic PCR. Primers were designed such that the amplified insert contained sufficient upstream (540 bp) and downstream (1050 bp) regions to ensure proper expression of the gene. Restriction sites were introduced into the primers to facilitate cloning of the amplification product (pBJ8793) (Figure 3A). The cloned insert was able to complement the CpY deficiency of the Δ*pth1::HIS3* mutant as examined by the CpY plate assay.

Phenotypic consequences of the deletion of the *PTH1* gene: As was seen for *PEP12*, deletion of *PTH1* also conferred sensitivity to high levels of divalent cations. The Δ*pth1* mutant was sensitive to growth in medium containing Zn^{2+} (>5 mm), Ca^{2+} (>400 mm), Sr^{2+} (>500 mm), Mn^{2+} (>5 mm) or Li^{2+} (>100 mm) at both 30° and 37°. Interestingly, however, extended incubation for a period greater than 72 hr resulted in growth. In contrast, *pep12* mutants never overcome sensitivity to the presence of divalent cations in the growth medium even after an extended incubation (Becherer *et al.* 1996). Growth of the Δ*pth1* mutant was retarded in medium buffered at pH 7.

To evaluate the effects of Pth1p deficiency on vacuolar protein sorting, we performed kinetic studies of hydrolase maturation and targeting to the vacuole using spheroplasts of wild-type and Δ*pth1::HIS3* strains. Wild-type cells completely processed the CpY precursor to mature CpY during the 20 min pulse and 30 min chase, indicating that CpY was properly delivered to the vacuole (Figure 5, lane 1). In contrast, in the Δ*pth1* strain, most CpY remained in its Golgi-modified precursor form, P2CpY, and was retained within the cell; little was recovered in the extracellular secreted fraction (Figure 5, lanes 3 and 4). A modest amount of processing of the precursor to mature form was also observed, which is consistent with the intermediate CpY plate assay phenotype. The Δ*pth1* mutant proved to be defective in maturation of two additional lumenal hydrolases, PrA and PrB. For both enzymes, wild-type cells processed PrA and PrB precursors to their mature forms during the 20 min pulse and 30 min chase (Figure 5, lane 1). In the Δ*pth1* mutant, PrA and PrB were recovered in their Golgi-modified precursor forms: proPrA (P2PrA) and proPrB (P3PrB). As was seen for CpY, however, the Golgi-modified PrA and PrB precursors remained primarily within the cell; they were recovered in the intracellular spheroplast fraction (Figure 5, lane 3). Thus, kinetic experiments indicate that the Δ*pth1* mutant is defective in delivery of soluble vacuolar hydrolases to the vacuole. Processing of the type

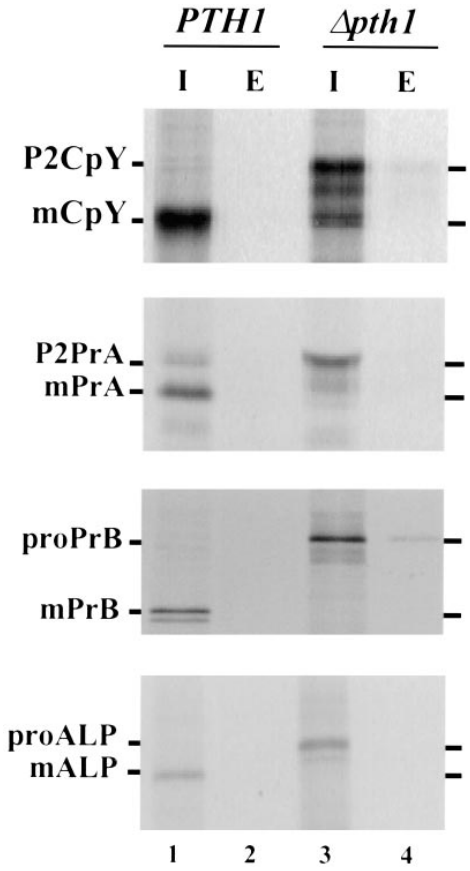

Figure 5.—Sorting and processing of vacuolar hydrolases. Spheroplasts of *PTH1* (BJ6252) and Δ*pth1::HIS3* (BJ8776) were pulse labeled with Trans^{35}S for 20 min and chased for 30 min at 30°. The labeled cultures were separated into spheroplast (**I**nternal) and medium (**E**xternal) fractions. Vacuolar hydrolases CpY, PrA, PrB and ALP were immunoprecipitated from each fraction, subjected to SDS-PAGE (ALP, 8.5%; CpY and PrA, 10%; PrB, 12%) followed by autoradiography. The positions of Golgi-modified precursors (P2CpY, proPrA, proPrB and proALP) and mature forms are indicated.

II vacuolar membrane hydrolase ALP was also blocked (Figure 5, lane 3). In the above-mentioned time course the Δ*pth1* mutant accumulated proALP in the intracellular fraction. Thus, deletion of *PTH1* causes a defect in the processing of both soluble and membrane hydrolases.

Vacuolar morphology of the Δ*pth1* mutant: To assess the vacuolar morphology in cells lacking the *PTH1* gene product, we subjected wild-type and Δ*pth1* cells to electron microscopy to examine vacuolar structures. The wild-type cell exhibits normal vacuolar structures with two to three lobes and one to three vacuoles per cell (Figure 6A). Δ*pth1* mutant cells exhibit "fragmented" vacuoles (five to six small, ellipsoidal vesicular structures) (Figure 6B). The cytoplasm of the Δ*pth1* mutant appeared more dense and granular compared with that of the wild-type strain. Furthermore, closer examination of the electron micrographs of the Δ*pth1* mutant strain revealed the presence of multiple small vesicles distributed throughout the cytoplasm (Figure 6, C and E, low magnification; Figure 6, D and F, high magnification). The vesicles measure approximately 40–60 nm in diameter and are indicated by arrows (Figure 6, D and F).

Epistatic relationship between *pep12* and *pth1*: To investigate the epistatic relationship between the two syntaxins, near isogenic *pep12::LEU2* (BJ8922) and Δ*pth1::HIS3* (BJ8771) strains were crossed and tetrads dissected. Using the ability to process and deliver CpY to the vacuole as a measure, epistasis was examined at two levels—by the CpY plate assay and by kinetic *in vivo* labeling experiments. For the CpY plate assay, spores from a single tetratype tetrad were streaked out on YPD plates along with controls. Cells were grown at both 30° and 37° for at least 48 hr before carrying out the test. At 30°, the wild-type strain tested red and was thus Cpy$^+$. The *pep12::LEU2* strain tested white or Cpy$^-$, indicating a deficiency in CpY activity. The Δ*pth1::HIS3* strain also exhibited a CpY deficiency, although it was less severe than that of the *pep12* mutant strain. The *pep12::LEU2* Δ*pth1::HIS3* double mutant displayed a CpY activity phenotype more like that of a *pep12* mutant than a *pth1* mutant. Raising the temperature to 37° did not cause any change in the CpY activity phenotypes. However, the double mutant exhibited a synthetic growth defect and was unable to grow at 37° (Figure 7A).

The epistatic relationship was examined kinetically by assessing the ability of cells to correctly process and deliver CpY to the vacuole using spheroplasts of spore clones from the tetratype tetrad. During a 20 min pulse and 30 min chase, the wild-type strain processed the CpY precursor to its mature form, indicating proper delivery to the vacuole (Figure 7B, lane 1). As observed earlier, the Δ*pth1::HIS3* mutant accumulated most of the precursor, P2CpY, intracellularly (Figure 7B, lanes 3 and 4). In the *pep12::LEU2* mutant almost all P2CpY was secreted into the extracellular medium fraction (Figure 7B, lanes 5 and 6). In the *pep12::LEU2* Δ*pth1::HIS3* double mutant, CpY accumulated in its Golgi-modified precursor form, P2CpY, and almost all of it was secreted into the extracellular medium fraction (Figure 7B, lanes 7 and 8). The CpY maturation phenotype of the double mutant is like that of the *pep12* mutant, indicating that *pep12* is epistatic to *pth1* with respect to the CpY secretion phenotype.

Subcellular fractionation of Pth1p: To examine the intracellular location of Pth1p, we constructed an HA-tagged version of the gene. Four copies of the 9 amino acid HA epitope were introduced at the N-terminus of Pth1p by cloning (see materials and methods and Table 2). *PTH1::HA* was able to fully complement the CpY deficiency of the Δ*pth1::HIS3* mutant (Figure 3C, pBJ9100). Monoclonal antibodies that recognize this epitope tag precipitated a Pth1::HAp-specific protein in extracts prepared from cells carrying this construct, but not from cells lacking this construct (Figure 8A, lanes 1 and 2).

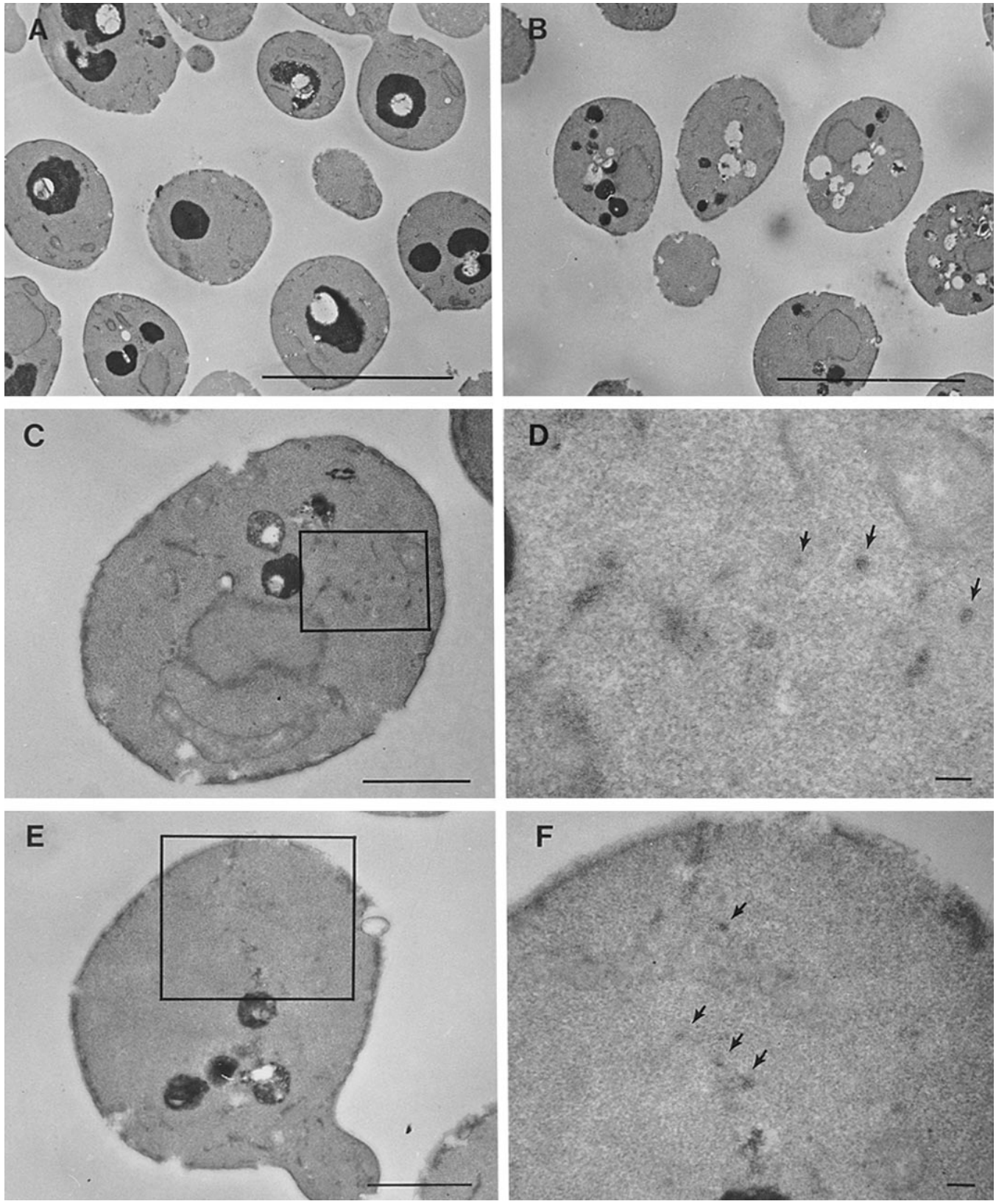

Figure 6.—Vacuolar morphology and vesicle accumulation in the Δ*pth1::HIS3* mutant. Strains were prepared and stained for electron microscopy as described in materials and methods. (A) *PTH1* (BJ6252), (B) Δ*pth1::HIS3* (BJ8776). Scale bars, 5 μm. (C–F) Accumulation of 40–60 nm vesicles in the Δ*pth1* (BJ8776) mutant. (C and E) Low magnification views. Scale bars, 1 μm. Insets shown at higher magnification in D and F, respectively. Scale bars, 100 nm. Arrows indicate vesicles observed.

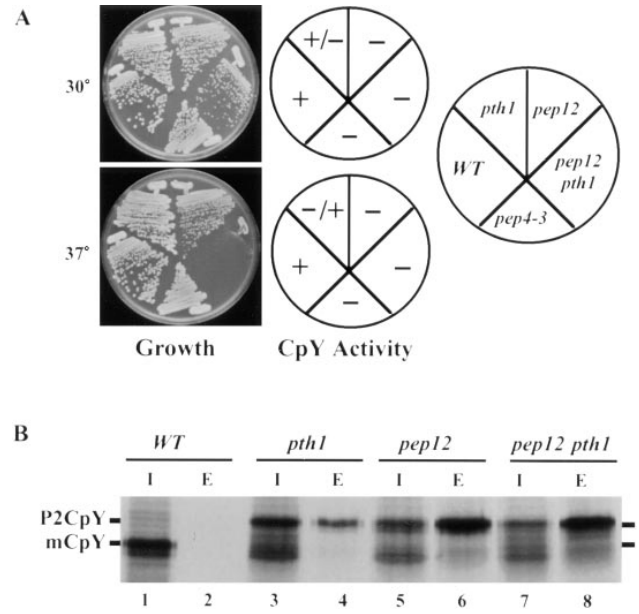

Figure 7.—Analysis of epistasis between *pep12* and *pth1*. Meiotic segregants in a tetratype tetrad obtained from a cross between near isogenic *pep12* (BJ8922) and *pth1* (BJ8771) strains were used for all epistasis experiments: *WT* (BJ8926), Δ*pth1::HIS3* (BJ8927), *pep12* (BJ8928) and Δ*pth1::HIS3 pep12* (BJ8929). (A) Viability was examined in addition to CpY activity by CpY (APE overlay) plate assay at both 30° and 37°. (B) Kinetic analysis of epistasis by examination of CpY sorting and processing. Spheroplasts of above-mentioned strains were pulse labeled *in vivo* with Trans^{35}S for 20 min and chased for 30 min at 30°. The labeled cultures were separated into spheroplast (**I**nternal) and medium (**E**xternal) fractions. CpY was immunoprecipitated from each fraction, subjected to SDS-PAGE (10%) followed by autoradiography. The positions of Golgi modified precursor P2CpY and mature form are indicated.

Radiolabeled cell extracts were subjected to differential centrifugation to separate various organelles on the basis of velocity sedimentation as described in Becherer *et al.* (1996). Lysates were fractionated by centrifugation into a 13,000 × *g* pellet (P13), a 100,000 × *g* pellet (P100) and a 100,000 × *g* supernatant (S100). Each fraction was examined for the presence of Pth1::HAp and the marker proteins—ALP (vacuole membrane), Pep12p (prevacuole/endosome), Kex2p (late-Golgi membrane) and G6PDH (cytosol)—by immunoprecipitation followed by SDS-PAGE and fluorography.

Nearly all of the vacuolar protein ALP was found in the P13 fraction (Figure 8B, lane 1). Most of Pep12p was found in the P13 fraction (Figure 8B, lane 1), which is consistent with its location in the endosome, a compartment similar, but not identical, to the vacuole, and one that is difficult to separate biochemically from the vacuole, as reported earlier (Becherer *et al.* 1996). Most of Kex2p was found in the P100 fraction (Figure 8B, lane 3) and G6PDH in S100 (Figure 8B, lane 2). Almost all of Pth1p was found in the P13 fraction (Figure 8B, lane 1). Along with the mutant phenotypes described above, especially the epistasis relationship between *pep12* and *pth1*, this localization is consistent with Pth1p being resident in vacuolar membranes.

Lumenal hydrolase profile under steady state conditions: To examine the processing of the lumenal hydrolases under steady-state conditions, we prepared whole-cell protein extracts from the spore clones of the above-mentioned tetrad grown to stationary phase. Presence and forms of vacuolar hydrolases were examined by immunoblot. Under steady-state conditions, the soluble hydrolases PrA, PrB and CpY were all processed to their mature forms in the *Δpth1* mutant, like the wild type. However the levels of the mature forms were reduced by almost 50% as compared to wild type (Figure 9, lane 2). Little or no antigen (pro or mature form) was observed in the *pep12* mutant extracts (Figure 9, lane 3) (Becherer *et al.* 1996). The phenotype of the *pep12 pth1* double mutant was identical to that of the *pep12* mutant (Figure 9, lane 4), in agreement with the epistasis relationship.

Steady-state processing of ALP: The precursor of the integral membrane hydrolase ALP is activated by proteolytic cleavage at the vacuole (Jones *et al.* 1982; Zubenko *et al.* 1982; Klionsky and Emr 1989). Processing of the ALP precursor was examined by immunoblot on whole-cell protein extracts prepared from strains constituting the tetratype tetrad used earlier for the epistasis experiments. In contrast to the soluble hydrolases, ALP underwent little or no processing in the Δ*pth1* mutant and accumulated in its pro form (Figure 10, lane 2). Almost all of the ALP precursor was processed to its mature form in the *pep12* mutant (Figure 10, lane 3) consistent with the use of a Pep12p independent pathway of vacuolar delivery, as has been recently proposed (Cowles *et al.* 1997; Webb *et al.* 1997). In the *pep12 pth1* double mutant, processing of the ALP precursor remained blocked, just as it was in the Δ*pth1* mutant (Figure 10, lane 4), suggesting that *pth1* is epistatic to *pep12* with respect to the ALP maturation phenotype.

Steady-state processing of ApI: The vacuolar hydrolase ApI utilizes an extrasecretory route from the cytoplasm to the vacuole, where it is proteolytically activated in a PrB-dependent fashion (Klionsky *et al.* 1992). Studies on translocation of ApI to the vacuole have defined a novel cytoplasm-to-vacuole targeting (Cvt) pathway (Harding *et al.* 1995). To examine whether this pathway was affected by the absence of Pth1p, we assessed processing of the ApI precursor by immunoblot on whole-cell protein extracts prepared from strains constituting the above-mentioned tetratype tetrad. Under steady-state conditions in the Δ*pth1* mutant, ApI accumulated in its precursor form and very little if any processing to the mature form was observed (Figure 10, lane 2). In the *pep12* mutant, ApI processing appeared to occur, albeit at a slower rate; approximately equal levels of pro and mature forms

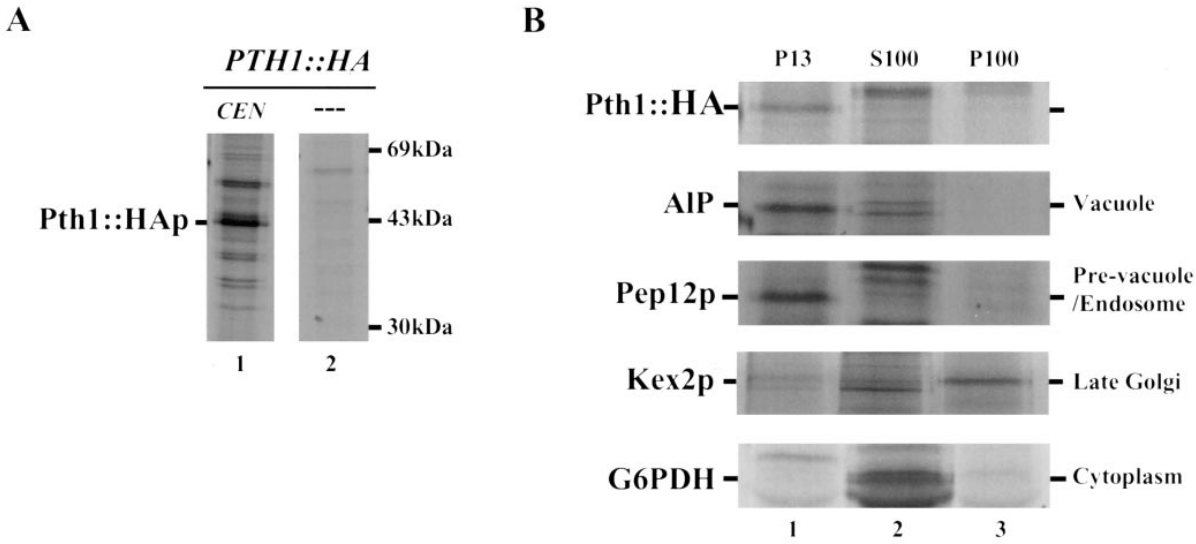

Figure 8.—Subcellular fractionation of Pth1p. (A) Spheroplasts of strain BJ8771 transformed with pBJ9100 (*PTH1::HA*/*CEN*) were pulse labeled *in vivo* with Trans^{35}S for 30 min and chased for 30 min at 30°. The spheroplast were lysed and Pth1::HAp was immunoprecipitated from the labeled cell extracts with monoclonal antibody that recognizes the HA epitope (12CA5). The precipitated protein was separated on a 12% acrylamide gel and subjected to autoradiography. The position of the epitope-tagged Pth1p is indicated. (B) Sixty OD_{600} units of spheroplasts of strain BJ8771 carrying plasmid pBJ9100 were pulse labeled *in vivo* with Trans^{35}S for 30 min and chased for 45 min at 30°. The spheroplasts were lysed and fractionated by differential centrifugation. First, the lysate was subjected to centrifugation at 13,000 × *g*, yielding a low-speed pellet (P13) and a low-speed supernatant fraction. The supernatant fraction was subjected to a second centrifugation at 100,000 × *g* resulting in a high-speed pellet and (P100) and a high-speed supernatant (S100). Pth1:HAp was immunoprecipitated from each one of the indicated fractions, as were the following organelle marker proteins: mALP (vacuole), Pep12p (prevacuole/endosome), Kex2p (late Golgi) and G6PDH (cytoplasm).

were observed (Figure 10, lane 3). Failure to process all of the ApI precursor could be the result of the low levels of active PrA and PrB under steady-state conditions. In the *pep12 pth1* double mutant, however, no processing of the ApI precursor was observed—all of the ApI accumulated in the precursor form, a phenotype the same as that of the *pth1* mutant (Figure 10, lane 4), suggesting that *pth1* is epistatic to *pep12* with respect to ApI maturation.

Vacuolar morphology by 6-CFDA accumulation: Vacuolar morphology was also examined by Nomarski and FITC optics after incubation of cells in 6-CFDA; free 6-CF, accumulates in the acidic vacuole as a charged fluorescent molecule (Preston *et al.* 1989). The wild-type strain displayed the normal vacuolar structures with two to three lobes and one to two vacuoles per cell (Figure 11, A and B). As mentioned earlier, the *pth1* mutant exhibited "fragmented" vacuolar structures (Figure 11, C and D). The *pep12* mutation results in a single large vacuole (Figure 11, E and F) (Becherer *et al.* 1996). The *pth1 pep12* double mutant exhibited "fragmented" vacuoles like the *pth1* mutant (Figure 11, G and H). With respect to this vacuolar morphology defect, *pth1* appears to be epistatic to *pep12*.

DISCUSSION

In this study we report the identification and characterization of Pth1p, a syntaxin/t-SNARE homolog involved in the delivery of hydrolases to the yeast vacuole. Pth1p was initially identified as a homolog of Pep12p, the prevacuolar/endosomal syntaxin that mediates docking and/or fusion of Golgi-derived transport vesicles (Becherer *et al.* 1996). We propose that Pth1p is the vacuolar syntaxin/t-SNARE homolog that facilitates docking and/or fusion reactions of transport vesicles at the vacuolar membrane (Figure 12). This conclusion is based on the examination of phenotypic consequences

TABLE 2

Plasmids

Plasmid	Insert	Vector
pBJ8793	*PTH1 Eco*RI/*Bam*HI fragment	pRS316 (*Eco*RI/*Bam*HI)
pBJ9100	*PTH1::HA* construct with native promoter region of *PTH1* inserted as *Xba*I/*Bam*HI fragment.	pRD54 GAL1::HA (pRS316 backbone)

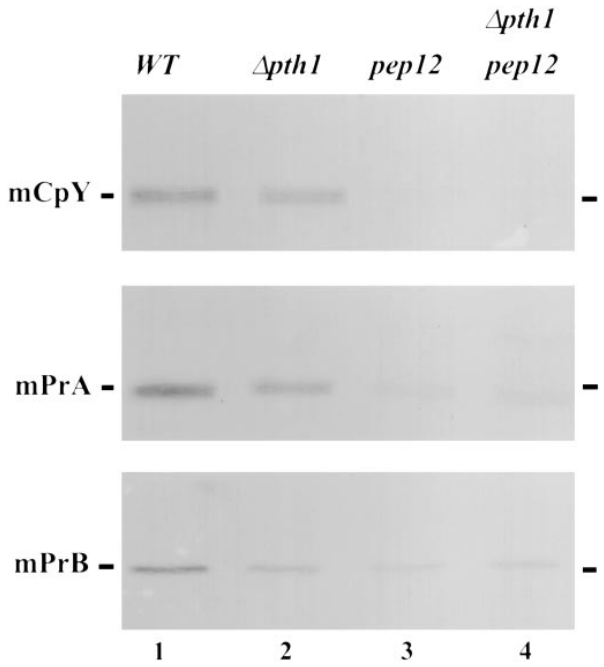

Figure 9.—Steady-state processing of lumenal hydrolases. Whole-cell protein extracts were prepared from *WT* (BJ8926), Δ*pth1::HIS3* (BJ8927), *pep12* (BJ8928) and Δ*pth1::HIS3 pep12* (BJ8929) and subjected to SDS-PAGE (per lane: CpY, 5 μg, 10% gel; PrA, 15 μg, 10% gel; PrB, 10 μg, 12% gel) followed by immunoblot analysis using affinity-purified polyclonal antibodies.

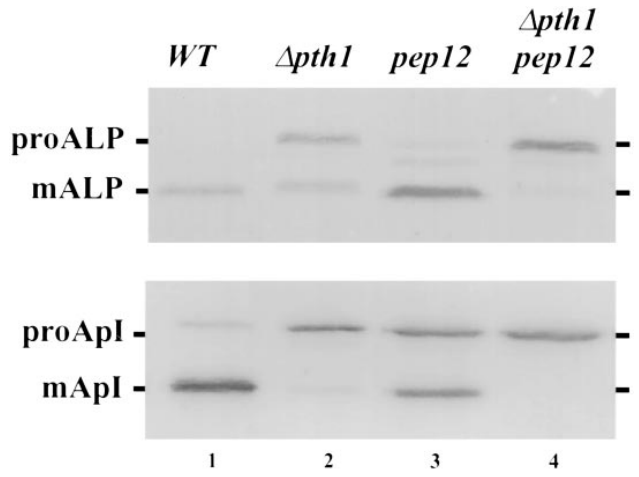

Figure 10.—ALP and ApI processing. Whole-cell protein extracts were prepared from *WT* (BJ8926), Δ*pth1::HIS3* (BJ8927), *pep12* (BJ8928) and Δ*pth1::HIS3 pep12* (BJ8929) and subjected to SDS-PAGE (per lane: ALP 50 μg, 10% gel; ApI, 15 μg, 10% gel) followed by immunoblot analysis using affinity-purified polyclonal antibodies.

of deletion of the *PTH1* gene, epistasis analyses between *pep12* and *pth1* mutations and the subcellular fractionation of Pth1p.

PTH1 (YOR106w) was identified in a genome-wide search for new members of the yeast syntaxin family using the heptad repeat region from Pep12p, which is the most highly conserved region among members of the syntaxin/t-SNARE protein family. Pth1p was predicted to be almost the same size as Pep12p; like Pep12p, a type II integral membrane protein with the characteristic heptad repeat region, it is strongly predicted to form an α-helical coiled coil immediately upstream of the transmembrane domain (Pth1p is predicted to have an additional, more N-terminal, coiled-coil domain). Deletion of the *PTH1* ORF causes a deficiency in CpY activity, as assessed by the CpY (APE overlay) plate assay, but with a less severe phenotype than *pep12* mutants. Furthermore, *pth1* mutants are also sensitive to high concentrations of divalent cations and unable to grow on medium buffered at pH 7, all indicators of diminished vacuolar function (Hiller 1997; Webb *et al.* 1997). These phenotypes implicate Pth1p in the vacuolar protein targeting pathway, suggesting that it is indeed a functional homolog of Pep12p. However, despite the high sequence similarity, neither gene when overexpressed can replace the other (data not shown), indicating that Pep12p and Pth1p are not functionally interchangeable.

The absence of Pth1p disrupts processing of both lumenal and membrane hydrolases. The Δ*pth1* mutant displays kinetic defects in processing of the post-Golgi precursors of PrA, PrB, CpY and ALP. However, under steady-state conditions, reduced levels of the mature forms of only the lumenal hydrolases are present; the vacuolar membrane hydrolase ALP remains unprocessed. In the absence of Pep12p, no post-Golgi processing of lumenal hydrolases is observed, but the processing of the membrane hydrolase ALP is unimpaired (Becherer *et al.* 1996; Burd *et al.* 1997; Cowles *et al.* 1997). Thus, the effects of the loss of Pth1p function are less severe than for the loss of Pep12p for the lumenal hydrolases, but not for the membrane hydrolase ALP. The effect on the lumenal hydrolases certainly correlates with the intermediate CpY activity phenotype of the Δ*pth1* mutant in the CpY (APE overlay) plate assay, compared with the *pep12* mutant. Almost all of P2CpY is secreted by a *pep12* mutant (Becherer *et al.* 1996). This phenotype is shared by several other mutants blocked at the Golgi-to-endosome stage of the vacuolar protein translocation pathway like *pep7* (Webb *et al.* 1997) and *vps45* (Cowles *et al.* 1994). In contrast, the Δ*pth1* mutant secretes little CpY, suggesting that P2CpY has traveled deeper into the vacuolar pathway so as to preclude its diversion into the secretory bulk flow. This led us to hypothesize that Pth1p might function at a step farther along the vacuolar protein targeting pathway than Pep12p. The epistasis relationship between *pep12* and *pth1* was consistent with this hypothesis. The *pep12 pth1* double mutant secretes nearly all P2CpY, indicating that *pep12* is epistatic to *pth1* for the CpY secretion phenotype and suggesting that Pep12p functions upstream of Pth1p in the pathway. Furthermore, since Pep12p is resident in the endosome/prevacuole

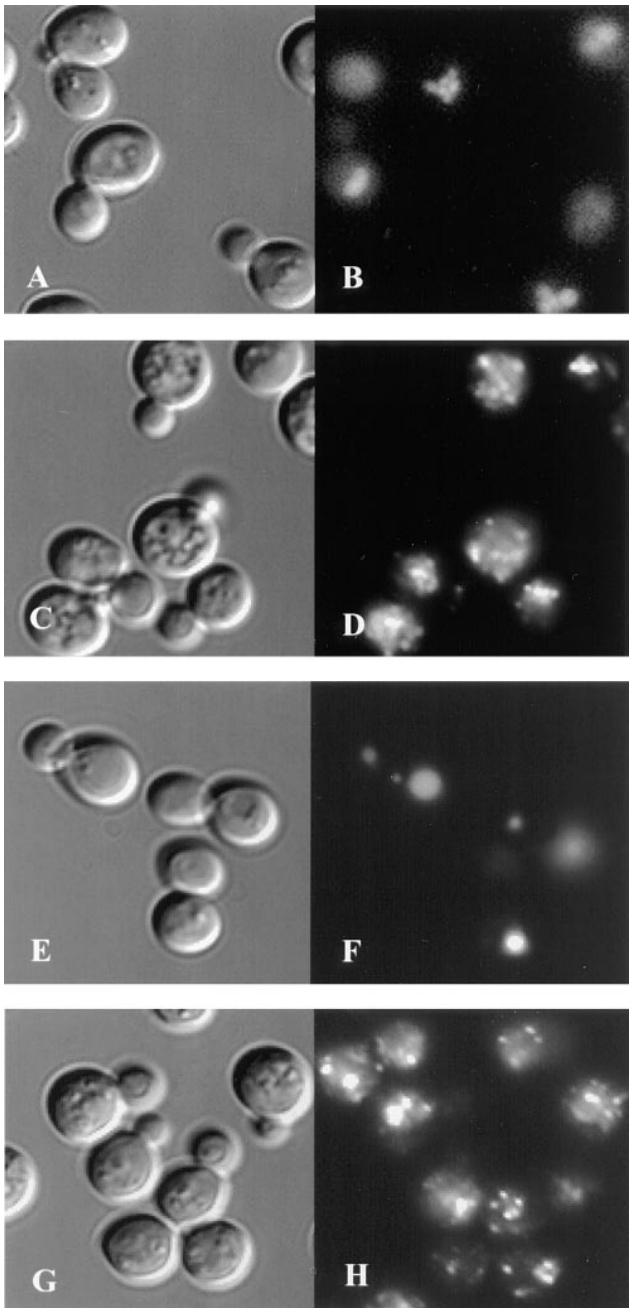

Figure 11.—(A and B) 6-CF accumulation in *WT* (BJ8926); (C and D) Δ*pth1::HIS3* (BJ8927); (E and F) *pep12* (BJ8928); and (G and H) Δ*pth1::HIS3 pep12* (BJ8929). Examined as described in materials and methods. Nomarski (A, C, E, G) and FITC (B, D, F, H) images are displayed.

(Becherer *et al.* 1996), Pth1p is an excellent candidate for a vacuolarly located syntaxin/t-SNARE. The results of subcellular fractionation studies on Pth1p confirmed the inferences from our genetic data. Subcellular fractionation by differential centrifugation demonstrated that Pth1p associated with a fraction enriched in vacuolar membranes as evidenced by the presence of the vacuolar integral membrane hydrolase, ALP.

Deletion of *PTH1* results in an abnormal vacuolar morphology; Δ*pth1* mutants display fragmented vacuolar structures, like the class B *vps* mutants (Raymond *et al.* 1992) and consistent with the identification of *pth1* as a vacuolar morphology mutant, *vam3* (Wada *et al.* 1992; Wada *et al.* 1997). These fragmented structures accumulate the vacuole specific dye 6-CF, suggesting that some degree of vacuolar acidification is achieved (Preston *et al.* 1989). The *pep12* mutant has a single large vacuole (Becherer *et al.* 1996). The *pep12 pth1* double mutant, however, has a fragmented vacuole, suggesting that *pth1* is epistatic to *pep12* with respect to the vacuolar morphology defect. This epistasis relationship can be explained by hypothesizing that the *pth1* defect represents a defect in the fusion of vacuoles at the final step in the vacuolar assembly pathway in the single and double mutant. This hypothesis is entirely in agreement with the results of Nichols *et al.* (1997). Using an *in vitro* assay for estimating homotypic vacuolar fusion, Nichols *et al.* (1997) made the following relevant observations: (i) interaction between the t-SNARE Vam3/Pth1p and v-SNARE Nyv1p is absolutely required for homotypic vacuolar fusion; (ii) fusion is completely abolished in the absence of the t-SNARE Vam3/Pth1p; (iii) Δ*nyv1* mutants possess a single large vacuole, but the Δ*nyv1* Δ*vam3*/*pth1* double mutant displays fragmented vacuolar structures like the Δ*vam3*/*pth1* mutant, suggesting that the vacuolar morphology defect of the Δ*vam3*/*pth1* mutant is epistatic to that of the Δ*nyv1* mutant.

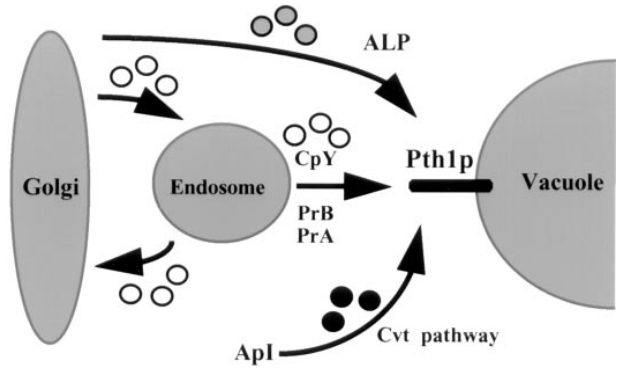

Figure 12.—Proposed site for Pth1p function. The presented observations of hydrolase sorting/transport defects along with protein localization data indicate that Pth1p is a multifunctional syntaxin/t-SNARE that participates in docking and/or fusion of transport vesicles arriving at the vacuolar membrane by at least three different routes: (1) endosome-derived transport vesicles carrying precursors of the lumenal hydrolases PrA, PrB and CpY; (2) Golgi-derived transport vesicles carrying the ALP precursor reaching the vacuole by an endosome-independent pathway; and (3) vesicles carrying the ApI precursor traveling to the vacuole directly from the cytoplasm by the Cvt pathway.

The accumulation of a 40–60 nm vesicle population in the Δ*pth1* mutant is consistent with a role for Pth1p in the vesicle consumption step of a vesicle-mediated transport pathway. Accumulation of vesicle populations of this size has been observed in the absence of the en-

dosomal syntaxin/t-SNARE, Pep12p (Becherer *et al.* 1996), and also at steps along the secretory pathway and its vacuolar branch (Novick *et al.* 1981; Newman and Ferro-Novick 1987; Shim *et al.* 1991; Cowles *et al.* 1994; Piper *et al.* 1994; Webb *et al.* 1997). Vesicles in this size range have been demonstrated to be transport vesicles ferrying proteinaceous cargo between intracellular organelles (Ferro-Novick and Jahn 1994; Rothman 1994); such vesicles are significantly smaller than the plasma membrane-directed secretory vesicles, which measure approximately 100 nm in diameter (Novick *et al.* 1981). Furthermore, in the absence of Pth1p, only the post-Golgi sorting and processing of vacuolar hydrolases are blocked. Taken together, these observations suggest that the vesicles that accumulate within the Δ*pth1* mutant originate from the vacuolar protein translocation pathway.

The vacuolar integral membrane hydrolase, ALP traverses the early secretory pathway *en route* to the vacuole, where it undergoes proteolytic maturation by PrA and/or PrB (Jones *et al.* 1982; Zubenko *et al.* 1982; Klionsky and Emr 1989). The post-Golgi processing and vacuolar delivery of ALP are unimpaired in a *pep12* mutant (Burd *et al.* 1997; Cowles *et al.* 1997). However, in the Δ*pth1* mutant, ALP maturation is blocked as assessed kinetically and also under steady-state conditions. This block in processing is not owing to the lack of active PrA and PrB, since under steady-state conditions mature forms of both hydrolases are present in the Δ*pth1* mutant. This implies that ALP is unable to localize to the same vesicular transport intermediates as active PrA and PrB, in addition to not being delivered to the vacuole. Recent evidence indicates that delivery of ALP to the vacuole normally occurs by a pathway that does not involve the prevacuole/endosome or the plasma membrane, and it has been suggested that ALP follows an alternative route directly from the Golgi to the vacuole (Cowles *et al.* 1997; Webb *et al.* 1997). Our findings are consistent with this suggestion. Furthermore, our observation that *pth1* is epistatic to *pep12* with respect to ALP maturation is also consistent with this proposed route, in that the *pep12*-induced block in the *pep12 pth1* double mutant is rendered irrelevant, resulting in an ALP maturation phenotype like that of the *pth1* mutant. The existence of parallel pathways for vesicular transport intermediates between two endomembrane organelles is not without precedent. Invertase and Pma1p have been shown to travel from the Golgi to the plasma membrane using distinct vesicle populations (Harsay and Bretscher 1995). However, the postulation of such parallel pathways begs the question: do common or separate sets of proteins exist to receive vesicles arriving by the two pathways? One suggested protein component for receiving ALP-bearing vesicles is Vam2/Vps41p. At the nonpermissive temperature a *vps41*^{tsf} mutant correctly processes and sorts the soluble hydrolase CpY and membrane hydrolase CpS, but maturation of ALP is blocked; furthermore, most of the ALP precursor is found in a subcellular fraction that contains primarily late-Golgi membranes (Cowles *et al.* 1997; Radisky *et al.* 1997). Vam2/Vps41p has been shown to exist in a complex with Vam6/Vps39p; this protein complex sediments in fractions enriched in vacuolar membranes (Nakamura *et al.* 1997). Both *vam2/vps41* and *vam6/vps39* mutants have a fragmented vacuole phenotype (class B morphology) like the Δ*pth1* mutant (Raymond *et al.* 1992; Nakamura *et al.* 1997). Mutations in *YPT7*, a Rab7 GTPase homolog, also result in phenotypes similar to those of the Δ*pth1* mutant: fragmented vacuolar morphology and a block in ALP maturation (Wichmann *et al.* 1992). However, mutations in *PTH1* and *YPT7* also affect maturation of the soluble hydrolases (this study; Wichmann *et al.* 1992), suggesting that their functions might extend into both Golgi-to-vacuole vesicular transport pathways.

The hydrolase ApI arrives at the vacuole via an extrasecretory route; the ApI precursor travels directly from the cytoplasm to the vacuole, where it undergoes maturation by PrB (Klionsky *et al.* 1992). The *cvt* mutants, which accumulate the ApI precursor, have identified protein components of this Cvt pathway (Harding *et al.* 1995). The oligomerization state of ApI before transport (Kim *et al.* 1997) and the requirement for a GTP-binding protein for ApI transport (Scott and Klionsky 1995) had suggested that ApI might utilize a vesicular mechanism for translocation into the vacuole. It has recently been demonstrated that the ApI precursor is indeed delivered to the vacuole in a "subvacuolar" vesicular intermediate (Scott *et al.* 1997). Scott *et al.* (1997) have suggested that the ApI-bearing transport vesicles might utilize SNARE-like components to ensure proper delivery to the vacuole. They speculate whether these transport vesicles are delivered directly to the vacuole or are instead delivered first to the late endosome and then to the vacuole by endosome maturation, as in mammalian cells (Dunn 1995). Our results shed some light on these speculations. We have observed that the Δ*pth1* mutant accumulates the cytoplasmic precursor of ApI despite the availability of active PrA and PrB. This implies, of course, that ApI does not travel in the same vesicles as PrA and PrB, but also suggests that Pth1p might be the syntaxin/t-SNARE required for docking and fusion of the ApI transport vesicles at the vacuolar membrane. The phenotypic similarity between *pth1* and *ypt7* mutants suggests that they might act at the same stage of the vacuolar pathway. *In vitro* reconstitution of the Cvt pathway has demonstrated a requirement for a GTP-binding protein for successful vacuolar delivery of ApI (Scott and Klionsky 1995). Our finding that ApI maturation is blocked in a Δ*ypt7* mutant (A. Srivastava and E. Jones, unpublished data) suggests that Ypt7p might be the Rab GTPase homolog involved in the vesicular delivery of ApI to the vacuole by the Cvt pathway. Furthermore, our

observations that ApI maturation is relatively unimpaired in a *pep12* mutant and that *pth1* is epistatic to *pep12* with respect to ApI maturation, suggest that the ApI transport vesicles might travel from the cytoplasm directly to the vacuole, bypassing the endosomal compartment.

Based on phenotypic similarities and/or sequence homology, there are few other gene products that might function at the same stage of the vacuolar pathway as Pth1p. Vps33/Pep14/Slp1p is one of the two nonredundant Sec1p homologs implicated in the vacuolar protein-sorting pathway, the other being Vps45p, which functions at the Golgi-to-endosome stage. Absence of Vps33/Pep14/Slp1p causes defects in hydrolase sorting and processing and also results in a vestigial vacuole phenotype (Jones 1977; Banta *et al.* 1990; Wada *et al.* 1990; Preston *et al.* 1992). We have found that *vps33/pep14/slp1* mutants are blocked in the maturation of ApI (A. Srivastava and E. Jones, unpublished data); however, this could be a secondary effect of the absence of any discernible vacuolar structures. There are no data suggesting that Vps33/Pep14/Slp1p participates in any docking/fusion steps in the vacuolar pathway. However, it remains the best candidate for the Sec1p homolog involved in the docking/fusion step at the vacuole. Mutations in another gene, *VAM7* (Wada *et al.* 1992), result in phenotypes similar to those seen in both *pth1* and *ypt7* mutants: fragmented vacuole morphology and reduced levels of CpY under steady-state conditions. Vam7p has limited sequence similarity to human SNAP-25 and SNAP-23 proteins. The reduced severity of the mutant phenotypes and its class B vacuolar morphology (Raymond *et al.* 1992; Wada *et al.* 1992), like those of the *pth1* mutant, make it a candidate SNAP-25 homolog at the vacuole rather than the endosome. Thus, within the framework of the SNARE hypothesis, we may have already identified a syntaxin/t-SNARE homolog (Pth1p), a Sec1p homolog (Vps33/Pep14/Slp1p), a SNAP-25 homolog (Vam7p) and a Rab GTPase homolog (Ypt7p) for vesicular docking/fusion reactions at the vacuolar membrane.

Taken together, our data suggest that Pth1p, a syntaxin/t-SNARE resident in the vacuolar membrane is a versatile protein with functions influencing several aspects of vacuolar biogenesis and trafficking. Pth1p function impinges on at least three biosynthetic routes of hydrolase delivery to the vacuole: endosome to vacuole, Golgi to vacuole and cytoplasm to vacuole. Furthermore, Pth1p appears to play a key role in vacuolar assembly, apparently by promoting fusion of several smaller vacuolar compartments.

We thank Joe Suhan for assistance with electron microscopy and Greg Fisher for help with fluorescence microscopy. We would like to thank members of the Jones laboratory for their helpful discussions throughout the course of this work. This research was supported by a grant from the National Institutes of Health (GM29713 to E.W.J.). The Center for Light Microscope Imaging and Biotechnology is a Science and Technology Center of the National Science Foundation, whose support (MCB-8920118) is acknowledged.

LITERATURE CITED

Bankaitis, V. A., L. M. Johnson and S. D. Emr, 1986 Isolation of yeast mutants defective in protein targeting to the vacuole. Proc. Natl. Acad. Sci. USA **83:** 9075–9079.

Banta, L. M., T. A. Vida, P. K. Herman and S. D. Emr, 1990 Characterization of yeast Vps33p, a protein required for vacuolar protein sorting and biogenesis. Mol. Cell. Biol. **10:** 4638–4649.

Baudin, A., O. Ozier-Kalogeropoulos, A. Denouel, F. Lacroute and C. Cullin, 1993 A simple and efficient method for direct gene deletion in *Saccharomyces cerevisae*. Nucleic Acids Res. **21:** 3329–3330.

Becherer, K. A., S. E. Rieder, S. D. Emr and E. W. Jones, 1996 Novel syntaxin homologue, Pep12p, required for the sorting of lumenal hydrolases to the lysosome-like vacuole in yeast. Mol. Biol. Cell **7:** 579–594.

Bennet, M. K., and R. H. Scheller, 1993 The molecular machinery for secretion is conserved from yeast to neurons. Proc. Natl. Acad. Sci. USA **90:** 2559–2563.

Birnboim, H., and J. Doly, 1979 A rapid alkaline extraction procedure for screening recombinant plasmid DNA. Nucleic Acids Res. **7:** 1513–1523.

Burd, C. G., M. Peterson, C. R. Cowles and S. D. Emr, 1997 A novel Sec18p/NSF-dependent complex required for Golgi-to-endosome transport in yeast. Mol. Biol. Cell **8:** 1089–1104.

Cepko, C. L., B. E. Roberts and R. C. Mulligan, 1984 Construction and applications of a highly transmissible murine retrovirus shuttle vector. Cell **37:** 1053–1062.

Cohen, C., and D. A. D. Parry, 1986 α-Helical coiled-coils: a widespread motif in proteins. Trends Biochem. Sci. **11:** 245–248.

Cooper, T. G., 1982 Transport in *Saccharomyces cerevisiae*, pp. 399–461 in *The Molecular Biology of the Yeast Saccharomyces: Metabolism and Gene Expression*, edited by J. N. Strathern, E. W. Jones and J. R. Broach. Cold Spring Harbor Laboratory, Cold Spring Harbor, NY.

Cowles, C. R., S. D. Emr and B. F. Horazdovsky 1994 Mutations in the *VPS45* gene, a *SEC1* homologue, result in vacuolar protein sorting defects and accumulation of membrane vesicles. J. Cell. Sci. **107:** 3449–3459.

Cowles, C. R., W. B. Snyder, C. G. Burd and S. D. Emr, 1997 Novel Golgi to vacuole delivery pathway in yeast: identification of a sorting determinant and required transport component. EMBO J. **16:** 2768–2782.

Dunn, T., K. Gable and T. Beeler, 1994 Regulation of cellular Ca^{2+} by yeast vacuoles. J. Biol. Chem. **269:** 7273–7278.

Dunn, W. A., 1995 Autophagy and related mechanisms of lysosome mediated protein degradation. Trends Cell. Biol. **4:** 139–143.

Ferro-Novick, S., and R. Jahn, 1994 Vesicle fusion from yeast to man. Nature **370:** 191–193.

Harding, T. M., K. A. Morano, S. V. Scott and D. J. Klionsky, 1995 Isolation and characterization of yeast mutants in the cytoplasm to vacuole protein targeting pathway. J. Cell Biol. **131:** 591–602.

Harsay, E., and A. Bretscher, 1995 Parallel secretory pathways to the cell surface in yeast. J. Cell Biol. **131:** 297–310.

Hawthorne, D., and R. Mortimer, 1960 Chromosome mapping in *Saccharomyces cerevisiae*: centromere-linked genes. Genetics **45:** 1085–1110.

Hill, J., K. A. Ian, G. Donald and D. Griffiths, 1991 DMSO-enhanced whole cell yeast transformation. Nucleic Acids Res. **19:** 5791.

Hiller, M. A., 1997 Isolation and characterization of mutants defective in the Ca^{2+} homeostasis in the yeast *Saccharomyces cerevisiae*. Ph.D. Thesis, Carnegie Mellon University, Pittsburgh.

Hoffman, C. S., and R. Winston, 1987 A ten-minute DNA preparation from yeast efficiently releases autonomous plasmids for transformation of *Escherichia coli*. Gene **57:** 267–272.

Jones, E. W., 1977 Proteinase mutants of *Saccharomyces cerevisiae*. Genetics **85:** 23–33.

Jones, E. W., 1991 Three proteolytic systems in the yeast *Saccharomyces cerevisiae*. J. Biol. Chem. **266:** 7963–7966.

Jones, E. W., and D. G. Murdock, 1994 Proteolysis in the yeast vacuole, pp. 115–134 in *Cellular Proteolytic Systems*, edited by A. J. Ciechanover and A. L. Schwartz. Wiley-Liss, New York.

Jones, E. W., G. S. Zubenko and R. R. Parker, 1982 *PEP4* gene function is required for expression of several vacuolar hydrolases in *Saccharomyces cerevisiae*. Genetics 102: 665–677.

Jones, E. W., C. A. Woolford, C. M. Moehle, J. A. Noble and M. I. Innis, 1989 Genes, zymogens, and activation cascades of yeast vacuolar proteases, pp. 141–147 in *Cellular Proteases and Control Mechanisms: Proceedings of a Glaxo–UCLA Colloquium on Cellular Proteases and Control Mechanisms*, edited by T. E. Hugli. Wiley-Liss, New York.

Jones, E. W., G. C. Webb and M. A. Hiller, 1997 Biogenesis and function of the yeast vacuole, pp. 363–470 in *Molecular and Cellular Biology of the Yeast Saccharomyces: Cell Cycle and Cell Biology*, edited by J. R. Pringle, J. R. Broach and E. W. Jones. Cold Spring Harbor Laboratory Press, Cold Spring Harbor, NY.

Kim, J., S. V. Scott, M. N. Oda and D. J. Klionsky, 1997 Transport of a large oligomeric protein by the cytoplasm to vacuole protein targeting pathway. J. Cell Biol. **137:** 609–618.

Klionsky, D. J., and S. D. Emr, 1989 Membrane protein sorting: biosynthesis, transport and processing of yeast vacuolar alkaline phosphatase. EMBO J. **9:** 2241–2250.

Klionsky, D. J., R. Cueva and D. S. Yaver, 1992 Aminopeptidase I of *Saccharomyces cerevisiae* is localized to the vacuole independent of the secretory pathway. J. Cell Biol. **119:** 287–299.

Kyte, J., and R. Doolittle, 1982 A simple method for displaying the hydropathic character of a protein. J. Mol. Biol. **157:** 105–132.

Lupas, A., M. Van Dyke and J. Stock, 1991 Predicting coiled-coils from protein sequences. Science **252:** 1162–1164.

McLachlan, A. D., and J. Karn, 1982 Periodic charge distribution in the myosin rod amino acid sequence match cross bridge spacings in muscle. Nature **229:** 226–231.

McLachlan, A. D., and M. Stewart, 1975 Tropomyosin coiled-coil interactons: evidence for an unstaggered structure. J. Mol. Biol. **98:** 293–304.

Nakamura, N., A. Hirata, Y. Ohsumi and Y. Wada, 1997 Vam2/Vps41p and Vam6/Vps39p are components of a protein complex on the vacuolar membranes and are involved in vacuolar assembly in the yeast *Saccharomyces cerevisiae*. J. Biol. Chem. **272:** 11344–11349.

Newman, A. P., and S. Ferro-Novick, 1987 Characterization of new mutants in the early part of the yeast secretory pathway isolated by a [^{3}H]mannose suicide selection. J. Cell Biol. **105:** 1587–1594.

Nichols, B. J., C. Ungermann, H. R. B. Pelham, W. T. Wickner and A. Haas, 1997 Homotypic vacuolar fusion mediated by t- and v-SNAREs. Nature **387:** 199–202.

Nothwehr, S. F., E. Conibear and T. H. Stevens, 1995 Golgi and vacuolar membrane proteins reach the vacuole in *vps1* mutant yeast cells via the plasma membrane. J. Cell Biol. **129:** 35–46.

Novick, P., S. Ferro and R. Schekman, 1981 Order of events in the yeast secretory pathway. Cell **25:** 461–469.

Ohsumi, Y., and Y. Anraku, 1983 Calcium transport driven by a proton motive force in vacuolar membrane vesicles of *Saccharomyces cerevisiae*. J. Biol. Chem. **258:** 5614–5617.

Parry, D. A. D., 1982 Coiled-coils in alpha-helix-containing proteins: analysis of residue types within the heptad repeat and the use of these data in the prediction of coiled-coils in other proteins. Biosci. Rep. **2:** 1017–1024.

Piper, R. C., E. A. Whitters and T. H. Stevens, 1994 Yeast Vps45p is a Sec1p homologue required for the consumption of vacuole targeted, post-Golgi transport vesicles. Eur. J. Cell Biol. **65:** 305–318.

Preston, R. A., R. F. Murphy and E. W. Jones, 1989 Assay of vacuolar pH in yeast and identification of acidification-defective mutants. Proc. Natl. Acad. Sci. USA **86:** 7027–7031.

Preston, R. A., P. S. Reinagel and E. W. Jones, 1992 Genes required for vacuolar acidity in *Saccharomyces cerevisae*. Genetics **131:** 551–558.

Pryer, N. K., L. J. Wuestehube and R. Schekman, 1992 Vesicle-mediated protein transport. Annu. Rev. Biochem. **61:** 471–516.

Radisky, D. C., W. B. Snyder, S. D. Emr and J. Kaplan, 1997 Identification of *VPS41*, a gene required for vacuolar trafficking and the assembly of the yeast high affinity iron transport system. Proc. Natl. Acad. Sci. USA **94:** 5662–5666.

Raymond, C. K., I. Howald-Stevenson, C. A. Vater and T. H. Stevens, 1992 Morphological classification of the yeast vacuolar protein sorting mutants: evidence for a prevacuolar compartment in class E *vps* mutants. Mol. Biol. Cell **3:** 1389–1402.

Robinson, J. S., D. J. Klionsky, L. M. Banta and S. D. Emr, 1988 Protein sorting in *Saccharomyces cerevisiae*: isolation of mutants defective in the delivery and processing of multiple vacuolar hydrolases. Mol. Cell. Biol. **8:** 4936–4948.

Rothman, J. E., 1994 Mechanisms of intracellular protein transport. Nature **372:** 55–63.

Rothman, J. H., and T. H. Stevens, 1986 Protein sorting in yeast: mutants defective in vacuole biogenesis mislocalize vacuolar proteins into the late secretory pathway. Cell **47:** 1041–1051.

Rothman, J. H., I. Howald and T. H. Stevens, 1989 Characterization of genes required for protein sorting and vacuolar function in the yeast *Saccharomyces cerevisiae*. EMBO J. **8:** 2057–2065.

Sambrook, J., E. F. Fritsch and T. Maniatis, 1989 *Molecular Cloning: A Laboratory Manual*, Ed. 2. Cold Spring Harbor Laboratory Press, Cold Spring Harbor, NY.

Scott, S. V., and D. J. Klionsky, 1995 *In vitro* reconstitution of cytoplasm to vacuole pathway in yeast. J. Cell Biol. **131:** 1727–1735.

Scott, S. V., M. Baba, Y. Ohsumi and D. J. Klionsky, 1997 Aminopeptidase I is targeted to the vacuole by a nonclassical vesicular mechanism. J. Cell Biol. **138:** 37–44.

Serrano, R., 1991 Transport across yeast vacuolar and plasma membrane, pp. 523–585 in *The Molecular and Cellular Biology of the Yeast Saccharomyces: Genome Dynamics, Protein Synthesis, and Energetics*, edited by J. R. Broach, J. R. Pringle and E. W. Jones. Cold Spring Harbor Laboratory Press, Plainview, NY.

Shim, J., A. P. Newman and S. Ferro-Novick, 1991 The *BOS1* gene encodes an essential 27-kd putative membrane protein that is required for vesicular transport from the ER to the Golgi complex in yeast. J. Cell Biol. **113:** 55–64.

Sikorski, R. S., and P. Hieter, 1989 A system of shuttle vectors and yeast host strains designed for efficient manipulation of DNA in *Saccharomyces cerevisiae*. Genetics **122:** 19–27.

Stevens, T., B. Esmon and R. Schekman, 1982 Early stages in the yeast secretory pathway are required for transport of carboxypeptidase Y to the vacuole. Cell **30:** 439–448.

Sudhof, T. C., 1995 The synaptic vesicle cycle: a cascade of protein–protein interactions. Nature **375:** 645–653.

Urech, K., M. Durr, T. Boller, A. Wiemken and J. Schwencke, 1978 Localization of polyphosphate in vacuoles of *Saccharomyces cerevisiae*. Arch. Microbiol. **116:** 275–278.

Van den Hazel, H. B., M. C. Kielland-Brandt and J. R. Winther, 1996 Review: biosynthesis and function of yeast vacuolar proteases. Yeast **12:** 1–16.

Wada, Y., K. Kitamoto, T. Kanbe, K. Tanaka and Y. Anraku, 1990 The *SLP1* gene of *Saccharomyces cerevisiae* is essential for vacuolar morphogenesis and function. Mol. Cell. Biol. **10:** 2214–2223.

Wada, Y., Y. Ohsumi and Y. Anraku, 1992 Genes for directing vacuolar morphogenesis in *Saccharomyces cerevisiae*. J. Biol. Chem. **267:** 18665–18670.

Wada, Y., N. Nakamura, Y. Ohsumi and A. Hirata, 1997 Vam3p, a new member of syntaxin related protein, is required for vacuolar assembly in the yeast *Saccharomyces cerevisae*. J. Cell. Sci. **110:** 1299–1306.

Webb, G. C., J. Zhang, S. J. Garlow, A. Wesp, H. Riezman *et al.*, 1997 Pep7p provides a novel protein that functions in vesicle-mediated transport between the yeast Golgi and endosome. Mol. Biol. Cell **8:** 871–895.

Wichmann, H., L. Hengst and D. Gallwitz, 1992 Endocytosis in yeast: evidence for the involvement of a small GTP-binding protein (Ypt7p). Cell **71:** 1131–1142.

Wiemken, A., and M. Durr, 1974 Characterization of amino acid pools in the vacuolar compartment of *Saccharomyces cerevisiae*. Arch. Microbiol. **101:** 45–57.

Wiemken, A., M. Schellenberg and K. Urech, 1979 Vacuoles: the sole compartments of digestive enzymes in yeast (*Saccharomyces cerevisiae*)? Arch. Microbiol. **123:** 23–35.

Woolford, C. A., C. K. Dixon, M. F. Manolson, R. Wright and E. W. Jones, 1990 Isolation and characterization of *PEP5*, a gene essential for vacuolar biogenesis in *Saccharomyces cerevisiae*. Genetics **125:** 739–752.

Yoshihisa, T., and Y. Anraku, 1990 A novel pathway of import of α-mannosidase, a marker enzyme of vacuolar membrane, in *Saccharomyces cerevisiae*. J. Biol. Chem. **265:** 22418–22425.

Zubenko, G. S., F. J. Park and E. W. Jones, 1982 Genetic properties of mutations at the *PEP4* locus in *Saccharomyces cerevisiae*. Genetics **102:** 679–690.

Communicating editor: A. P. Mitchell